4. Conclusions

(i) A Langmuir–Blodgett trough with a diamond-shaped constant-perimeter barrier was reported. This had a number of advantages over other designs:

(a) it was mechanically relatively simple and easy to construct,
(b) the diamond was easy to remove and could be cleaned quickly,
(c) there were no entrapment sites,
(d) there were no surfaces in friction (rollers or sliding barriers) likely to generate particles within the active area of the trough,
(e) the entire system was mounted in a laminar-flow enclosure (class 10), housed within a clean room (class 1000), to keep particulate contamination to a minimum.

(ii) The trough produces excellent graphs of surface pressure against area per molecule; the latter is accurate to $<\pm 2\%$, the diamond area alone being accurate to better than $\pm 1.5\%$.

(iii) High-quality multilayer films may be deposited, free of gross ionic contamination and pinholes.

(iv) The flow patterns during deposition are acceptable (figure 6) when compared with those reported for conventional trough designs (Daniel and Hart 1985, Daniel *et al* 1985).

Acknowledgments

We would like to acknowledge the valuable early development of the diamond concept undertaken with Dr C P Lewis and Mr T K Hesketh, the skilful machining of Mr A J Cranston, the useful discussions with Dr R Sethi (Plessey, Caswell) and Dr I V F Viney, and the preliminary electrical studies by Mr S Sparrow.

References

Daniel M F and Hart J T T 1985 Effect of surface flow on the morphology of Langmuir–Blodgett films. *J. Mol. Electron.* **1** 97

Daniel M F, Dolphin J C, Grant A J, Kerr K E N and Smith G W 1985 A trough for the fabrication of non-centrosymmetric Langmuir–Blodgett films *Thin Solid Films* **133** 232

den Engelsen D 1971 Ellipsometry of anisotropic films *J. Opt. Soc. Am.* **61** 1460

Severn J K and Batchelder D N 1984 Vibration analysis of a Langmuir trough. *J. Phys. E: Sci. Instrum.* **17** 133

Tanguy J 1972 Study of metal–organic monolayer–semiconductor structures *Thin Solid Films* **13** 33

Thin Solid Films 1985 *(2nd Int. Conf. on LB films, Schenectady, USA)* **132–134**

Von Tscharner V and McConnell H M 1981 An alternative view of phospholipid phase behaviour at the air–water interface. Microscope and film balance studies. *Biophys. J.* **36** 409

J. Phys. E: Sci. Instrum. **21** (1988) 167–170. Printed in the UK

A low-cost, high-performance DC cold-wire bridge

Jon Haugdahl and John H Lienhard V
Department of Applied Mechanics and Engineering Sciences, University of California, La Jolla, CA 92093, USA

Received 3 March 1987, in final form 14 July 1987

Abstract. A simple design for a high-performance DC resistance thermometer bridge is presented. The bridge takes advantage of low-drift, low-offset operational amplifiers to obtain the low noise levels and flexibility previously available only from AC bridges. The characteristics of the bridge's performance are discussed and spectral measurements with the circuit are considered.

1. Introduction

Resistance-wire thermometery has been widely used for measurement of fluctuating temperature in turbulent flows since its introduction by Corrsin (1947) forty years ago. The operating principle of these sensors is that a very fine wire (typically $1\,\mu m$ diameter platinum) situated in a turbulent flow will follow the flow temperature closely up to frequencies of several kilohertz. The resistance of the wire varies in proportion to its temperature, and, by arranging the wire as one leg of a bridge circuit, this fluctuating resistance can be measured. Once calibrated, such a sensor can be used to measure turbulent temperature. These sensors are commonly referred to as *cold wires* (in contradistinction to the *hot wires* of anemometry) because the bridge current is always made so small as to produce negligible ohmic heating in the wire.

The bridge circuit is often a limiting factor in cold-wire experimentation. The amplifier and bridge current source must be free of drift and input noise. The circuit's frequency response must be at least as high as that of the sensor employed and the noise levels of the circuit must be low enough to resolve the RMS temperature of any flow of interest. The design of bridge circuits has evolved over the years in response to these difficulties.

The earliest circuits were DC Wheatstone bridges which used batteries as current sources and relied on external amplification. These bridges were generally replaced in the sixties and seventies by AC Wheatstone bridges (Gibson and Schwarz 1963, Yeh and Van Atta 1973) which suffered less drift and facilitated higher gains. The noise levels of the AC bridges were mK, depending on the choice of sensor and bridge current. Sophisticated forms of the AC temperature bridge have seen wide application in both laboratory and field studies.

In spite of their fine performance, the AC bridges suffer from the complexity and cost of the circuit; for many purposes a simpler bridge is desirable. One such design was presented by Tavoularis (1978). His circuit used a battery-referenced voltage-to-current converter to drive the cold wire and compared the sensor voltage with a reference to obtain an output proportional to the wire temperature fluctuation. The circuit was thus relatively simple – no AC components were employed – and had acceptably low noise levels. However, the circuit had the disadvantage of requiring a

0022-3735/88/020167+04 \$02.50

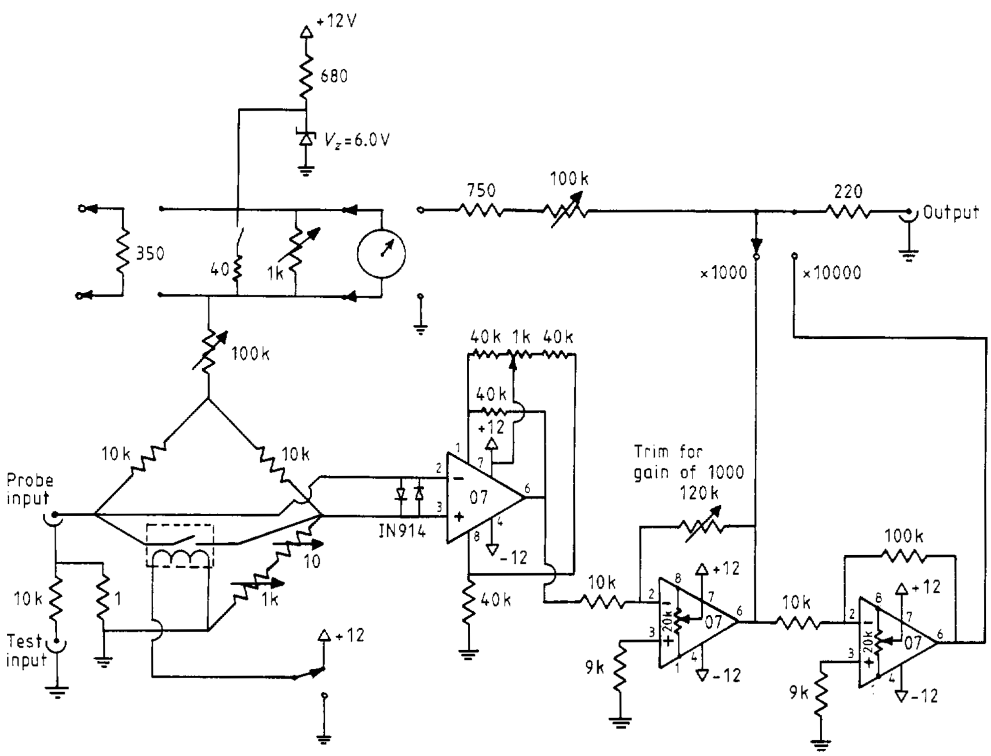

Figure 1. The bridge circuit.

high-quality external differential amplifier, and certain resistors had to be changed for different operating conditions. Hence, other approaches can still be explored profitably.

Current operational amplifier technology makes it possible to build a high-performance DC bridge which has *internal* amplification and which can achieve stability and noise levels equivalent to the AC bridges. Here we present a design for such a bridge. The circuit given is free of the complexity of the AC bridges as well as the drift and noise problems historically associated with integrated-circuit-based DC bridges.

2. The bridge circuit

Figure 1 shows the bridge circuit. The circuit is centred around a Wheatstone bridge, one leg of which is the cold-wire probe. The upper two legs are 10 kΩ precision resistors (0.01%) and the last leg is a pair of wire-wound trim pots, 1 kΩ and 10 Ω, which serve as coarse and fine bridge balances. Current is fed to the bridge from a 6 V source regulated by a temperature-compensated Zener diode. The current is adjusted with a 100 kΩ variable resistor and an intermediate switch which provides 100 μA and 500 μA meter ranges. The load above the sensor is sufficiently large that fluctuations in the sensor resistance have a negligible effect on the current.

A meter reads either bridge current or output voltage. When it is switched out of the current line, an equal resistance is switched into that line in its place. A potentiometer sits in parallel with the meter to trim its scale.

The voltage difference across the bridge is delivered to the inputs of a commercial-grade Precision Monolithics OP-07 amplifier†. This amplifier serves to buffer the output and provides the initial gain of the circuit. The amplifier is connected in a feedback configuration, summing at pin 1 rather than pin 2. This arrangement increases the input impedance at pin 2 so that the inputs are symmetrical with respect to the amplifier's internal circuitry. The common-mode rejection ratio is improved from 60 dB to more than 90 dB. Thus, the already low drift and noise levels of the amplifier are further enhanced. Such designs are discussed by Mortensen (1972) and Counts *et al* (1981).

The zero of the amplifier is adjusted by a variable resistor in conjunction with a reed relay zero check across the bridge. A pair of diodes across the inputs protect the amplifier. The output of this amplifier is sent to an additional pair of cascaded OP-07s for a final gain switchable between ×1000 and ×10 000.

Temperature drift error in the bridge circuit is minimised by using metal film resistors and identical connecting wires wherever possible. The components of the bridge were selected to have nearly identical temperature coefficients of resistance, so that the resistors track together if the bridge temperature changes. Cermet trim pots, if used, should be used in conjunction with metal film resistors which provide the bulk of the load. Efforts should be made to use a single metal for wiring ahead of the amplifier inputs to minimise uncancelled thermoelectric potentials; such potentials may produce minor DC offsets. Good construction technique must be used throughout.

The bridge is powered with a *remote* supply to minimise heating effects and 60 cycle noise. The supply uses conventional full-wave rectification into three-terminal regulators at ±12 V. The supply signal must be free of 60 cycle noise. The bridge itself should be kept at a distance from unshielded sources of magnetic field to avoid induced 60 cycle noise.

3. Bridge response and performance

For fluctuations of sensor resistance small compared with the

† The OP-07 is largely responsible for the success of this design because of its extremely low offset voltage (10 μV), low temperature drift (0.2 μV K^{-1}), high stability (0.2 μV/month), and low input noise. Two better grades of OP-07 are available, although we achieved good performance using the commercial grade.

upper bridge resistor, the circuit's output is

$$e = GI\Delta R_s \qquad (1)$$

where R_s is the sensor resistance, ΔR_s is the change from resistance at balance, G is the gain and I is the current through the sensor. The temperature dependence of sensor resistance is

$$R_s = R_{s0}(1 + \alpha_0(\theta - \theta_0)) \qquad (2)$$

for moderate variation of temperature θ (the subscript 0 denotes a reference state and α_0 is the temperature coefficient of resistivity). For such temperature changes, fluctuations in sensor resistance will be small enough that equation (1) holds and bridge output is related to the difference between sensor temperature and sensor temperature at balance by

$$e = GIR_{s0}\alpha_0\Delta\theta. \qquad (3)$$

The temperature response will be limited by the frequency response and noise levels of the circuit. The frequency response of the circuit was determined by injecting a sine wave at the test input on the bridge and measuring the output response. The result, presented in figure 2, shows a -3 dB point of 8.2 kHz. In most cases, the frequency response of this circuit will exceed the frequency response of the sensor, the latter being less than 5 kHz for all but the smallest wires (see, for example, LaRue *et al* 1975). The output noise of the circuit was measured with a fixed load connected in place of the probe. The unfiltered noise is 13.6 mV RMS, and with low-pass filtering at 5 kHz the noise is 8.5 mV RMS†.

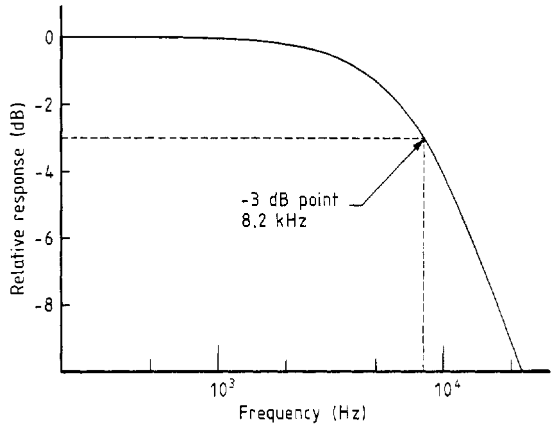

Figure 2. Frequency response of the bridge circuit.

The drift of the circuit was measured at a gain of 10 000 with metal-film resistor in place of the probe. The output was found to vary in a range of ± 10 mV at a rate not exceeding 4 mV h^{-1}, and the drift was not correlated with temperature shifts over the range of temperature fluctuations encountered in our laboratory (± 2 K). The bridge output saturates at $+11.2$ V and -10.5 V from which the operating range can be calculated using equation (3).

4. Spectral characteristics

To examine the spectral characteristics of the circuit, measurements were made in a turbulent grid flow with strong

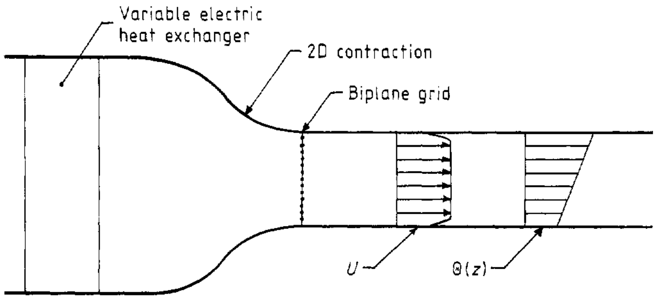

Figure 3. The thermally stratified wind tunnel: U = mean velocity; Θ = mean temperature; $\mathrm{d}\Theta/\mathrm{d}z = 199\,\mathrm{K\,m^{-1}}$.

thermal stratification as illustrated in figure 3 (see also Lienhard 1988). The mean flow speed was 2.4 m s^{-1} and the RMS turbulence intensity was 3% at the location of measurement. The cold-wire probe was a Dantec model 55P31 (1 μm diameter by 0.4 mm long platinum wire, $\sim 65\ \Omega$) driven at 230 μA.

Typical temperature power spectra are shown in figure 4. The upper curve is the temperature spectrum measured with thermal stratification (RMS θ of 1.93 K) and has classical form‡. The next curve down is the spectrum of the same flow without heating. The RMS temperature measured in this case was 0.011 K. The isothermal curve is 55 dB below the heated curve at lower frequencies and shows line noise at 60 cycles and its odd harmonics.

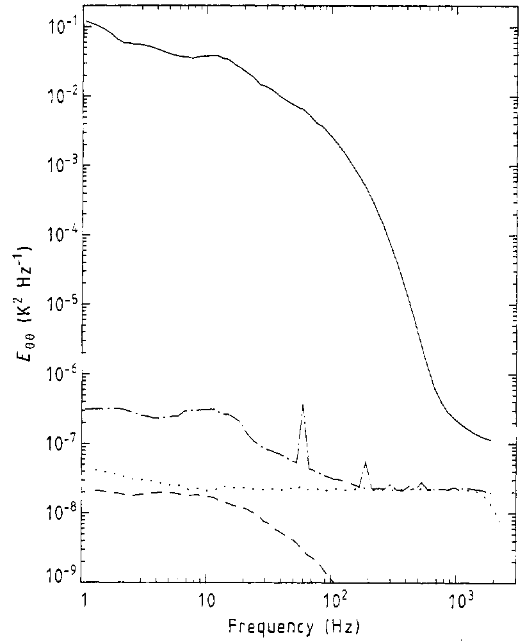

Figure 4. Temperature power spectra: ——, stratified flow; — · —, isothermal flow; ····, metal-film resistor; – – –, velocity contamination.

The 'isothermal' spectrum possesses enough structure that it is worthwhile to examine the nature of the output signal for this case. The probe was replaced with a metal-film resistor and the bridge output measured; this voltage was converted to an equivalent temperature noise for the 55P31 sensor using

† The equivalent temperature noise depends on the sensor current and resistance (diameter), with the lowest noise for higher currents and smaller sensor wire diameters. The objective of minimising noise must be balanced against the increased velocity sensitivity of the cold wire at higher currents and the greater fragility of smaller diameter sensors.

‡ This spectrum shows a high-frequency noise tail five-and-one-half decades below the peak caused by round-off error in the FFT calculation.

equation (3). The associated temperature spectrum is shown in figure 4 (RMS $\theta = 0.006$ K), and coincides with the high-frequency portion of the isothermal spectrum. Thus, the high-frequency end of the isothermal spectrum represents the noise limit of bridge sensitivity. The Johnson noise of the sensor (RMS $\theta = 7.5 \times 10^{-8}$ K) lies well below the observed noise limit, so the latter is purely electronic. The line noise spikes do not appear in the metal-film resistor spectrum and thus may be due to the electromagnetic pick-up of the cold wire itself.

To examine the low-frequency end of the isothermal signal, we may follow the general procedure of Wyngaard (1971) and compute the velocity-induced temperature signal. Wyngaard showed that

$$\theta - \theta^{\mathrm{m}} = \frac{I^2 R_s}{\overline{H}^2} \frac{\partial \overline{H}}{\partial U} u \tag{4}$$

where $\theta - \theta^{\mathrm{m}}$ is the difference between actual and measured fluid temperature, $\overline{H}$ is the time-averaged overall heat transfer coefficient for the wire, and u is the turbulent fluctuation in the mean velocity U. To compute $\overline{H}$ we use the equation of Nakai and Okazaki (1975):

$$\overline{H} = \frac{\pi l k}{0.8237 - \ln(Pe^{1/2})} \qquad Pe = Ud/\alpha < 0.2 \tag{5}$$

where l and d are the wire length and diameter, k and α are the thermal conductivity and diffusivity of air, and Pe is the Péclet number based on diameter. Differentiating with respect to U, we find

$$\theta - \theta^{\mathrm{m}} = -\underbrace{\frac{I^2 R_s}{2\pi l k U}}_{0.020\ \mathrm{K\,s\,m^{-1}}} u \tag{6}$$

where we have evaluated the coefficient for our flow.

Using equation (6) with the velocity spectrum measured in this flow, we obtain the velocity contamination spectrum shown in figure 4 (RMS $\theta = 0.001$ K). The contamination spectrum lies below both the isothermal and noise spectra. Apparently, the low-frequency structure of the isothermal temperature spectrum is a real temperature signal and cannot be attributed to velocity contamination.

Acknowledgments

The authors would like to thank K N Helland for helpful discussions of the spectral results. This work was supported by the National Science Foundation under grant no OCE85-11289.

References

Corrsin S 1947 Extended applications of the hot-wire anemometer
Rev. Sci. Instrum. **18** 469–71

Counts L, Kitchin C and Jung W 1981 Op amp + feedback = instrumentation amp
EDN **26** (7) 267

Gibson C H and Schwarz W H 1963 Detection of conductivity fluctuations in a turbulent flow field
J. Fluid Mech. **16** 357–64

LaRue J C, Deaton T and Gibson C H 1975 Measurement of high-frequency turbulent temperature
Rev. Sci. Instrum. **46** 757–64

Lienhard J H V 1988 Decaying turbulence in thermally stratified flow *Doctoral dissertation* University of California at San Diego

Mortensen H 1972 IC op amps make inexpensive instrumentation amplifiers
EDN **17** (10) 52

Nakai S and Okazaki T 1975 Heat transfer from a horizontal circular wire at small Reynolds and Grashof numbers – I Pure convection
J. Heat Mass Transfer **18** 387–96

Tavoularis S 1978 A circuit for the measurement of instantaneous temperature in heated turbulent flows
J. Phys. E: Sci. Instrum. **11** 21–3

Wyngaard J C 1971 The effect of velocity sensitivity on temperature derivative statistics in isotropic turbulence
J. Fluid Mech. **48** 763–9

Yeh T T and Van Atta C W 1973 Spectral transfer of scalar and velocity fields in heated-grid turbulence
J. Fluid Mech. **58** 233–61